THE JOURNAL OF BIOLOGICAL CHEMISTRY VOL. 286, NO. 49, pp. 42670–42678, December 9, 2011

Inhibitor of *Apoptosis* (IAP)-like Protein Lacks a Baculovirus IAP Repeat (BIR) Domain and Attenuates Cell Death in Plant and Animal Systems*[S]

Received for publication, May 18, 2011, and in revised form, September 15, 2011 Published, JBC Papers in Press, September 16, 2011, DOI 10.1074/jbc.M111.262204

Woe Yeon Kim[‡1], Sun Yong Lee[‡1,2], Young Jun Jung[‡1,2], Ho Byoung Chae[‡1,2], Ganesh M. Nawkar[‡], Mi Rim Shin[‡], Sun Young Kim[‡], Jin Ho Park[‡], Chang Ho Kang[‡], Yong Hun Chi[‡], Il Pyung Ahn[§], Dae Jin Yun[‡], Kyun Oh Lee[‡], Young-Myeong Kim[¶], Min Gab Kim[§‖3], and Sang Yeol Lee[‡4]

From the [‡]Division of Applied Life Science (BK21 Program), Gyeongsang National University, Jinju, 660-701, Korea, the [§]National Academy of Agricultural Science, RDA, Suwon 441-856, Korea, the [¶]Department of Molecular and Cellular Biochemistry, College of Medicine, Kangwon National University, Chunchon, Korea, and the [‖]College of Pharmacy, Gyeongsang National University, Jinju 660-751, Korea

A novel *Arabidopsis thaliana* inhibitor of apoptosis was identified by sequence homology to other known inhibitor of apoptosis (IAP) proteins. *Arabidopsis* IAP-like protein (AtILP) contained a C-terminal RING finger domain but lacked a baculovirus IAP repeat (BIR) domain, which is essential for anti-apoptotic activity in other IAP family members. The expression of *AtILP* in HeLa cells conferred resistance against tumor necrosis factor (TNF)-α/ActD-induced apoptosis through the inactivation of caspase activity. In contrast to the C-terminal RING domain of AtILP, which did not inhibit the activity of caspase-3, the N-terminal region, despite displaying no homology to known BIR domains, potently inhibited the activity of caspase-3 *in vitro* and blocked TNF-α/ActD-induced apoptosis. The anti-apoptotic activity of the AtILP N-terminal domain observed in plants was reproduced in an animal system. Transgenic *Arabidopsis* lines overexpressing *AtILP* exhibited anti-apoptotic activity when challenged with the fungal toxin fumonisin B1, an agent that induces apoptosis-like cell death in plants. In *AtIPL* transgenic plants, suppression of cell death was accompanied by inhibition of caspase activation and DNA fragmentation. Overexpression of *AtILP* also attenuated effector protein-induced cell death and increased the growth of an avirulent bacterial pathogen. The current results demonstrated the existence of a novel plant IAP-like protein that prevents caspase activation in *Arabidopsis* and showed that a plant anti-apoptosis gene functions similarly in plant and animal systems.

All living organisms use a process of cell suicide to achieve and maintain homeostasis during normal development as well as in response to environmental stress or during pathogen challenge (1). This functionally conserved process, known as programmed cell death (PCD)[5] or apoptosis, is genetically regulated and associated with distinct morphological and biochemical characteristics. Extensive study over the past decade has illuminated the biological and molecular mechanisms of the regulation of apoptosis in animal systems (2–7). Apoptosis is triggered by the sequential activation of cysteine proteases known as caspases, which results in protein cleavage and the breakdown of DNA molecules. This apoptotic cascade is regulated by both initiators and inhibitors and can be activated by diverse stimuli. Caspases are synthesized as zymogens that are activated by proteolytic cleavage at specific aspartic acid residues in the P1 position (8). Compartmentalization of caspases and their cofactors suggests that two major apoptotic pathways exist. One pathway of apoptosis, observed in animal systems, can be induced by the deprivation of serum from tissue culture cells, leading to the release of cytochrome *c* from mitochondria. Apoptosis activating factor-1 (Apaf1) and cytochrome *c* form a complex with procaspase-9, which is then activated. Active caspase-9 triggers the common caspase cascade by cleaving procaspase-3 (9–11). Caspase-3 is responsible either wholly or in part for the proteolytic cleavage of many key proteins, including poly(ADP-ribose) polymerase and lamin A (12–14). The existence of another apoptosis pathway derives from the observation that caspase-8 is activated when challenged with tissue necrosis factor (TNF-α) or Fas ligand (15–18). Loss of caspase activity is observed in cells that express the viral proteins CrmA, from cowpox, and p35, from baculovirus (19–23). Furthermore, overexpression of these viral caspase inhibitors in insect, nematode, and mammalian cells results in resistance to apoptosis, providing evidence that the components of the apoptotic pathway are highly conserved throughout evolution. This has led to speculation that functional equivalents of these viral proteins may exist in higher organisms.

The inhibitor of apoptosis (IAP) family of proteins plays a central role in apoptotic and inflammatory processes, conferring protection against cell death. IAP family members inter-

* This work was supported by the RDA for the Next-Generation BioGreen Program (SSAC; Grant PJ008109), by Cooperative Research Program for Agriculture Science and Technology Development Project PJ007850, and by MOEST for the WCU Program R32-10148.

[S] The on-line version of this article (available at http://www.jbc.org) contains supplemental Figs. 1 and 2.

[1] These authors contributed equally to this work.

[2] Supported by the BK21 Program, Korea.

[3] To whom correspondence may be addressed. Fax: 82-55-772-8289; E-mail: mgk1284@gnu.ac.kr.

[4] To whom correspondence may be addressed. E-mail: sylee@gnu.ac.kr.

[5] The abbreviations used are: PCD, programmed cell death; *p*NA, *p*-nitroanilide; MS, Murashige and Skoog; IAP, inhibitor of apoptosis; BIR, baculovirus IAP repeat; HR, hypersensitive response; Pph, *Pseudomonas syringae* pv. *phaseolicola*; Pma, *P. syringae* pv. *maculicola*; smGFP, soluble modified green fluorescent protein.

fere with the transmission of intracellular death signals by inhibiting caspase-dependent apoptotic pathways. The IAP proteins were initially identified in baculovirus as factors that prevented host cell apoptosis, allowing time for the virus to replicate (24, 25). Since then, eight mammalian IAPs (XIAP, HIAP1, HIAP2, ILP2, MLIAP, NAIP, BRUCE, and survivin) and three *Drosophila* IAP homologs (DIAP1, DIAP2, and Deterin) have been identified (26–35). IAP proteins exhibit a modular structure characterized by the presence of one or more baculovirus IAP repeat (BIR) domains. The BIR domain is a zinc-binding fold of ~70 amino acid residues that is essential for the anti-apoptotic properties of IAP proteins. The fact that all known IAP members have a BIR domain suggests that this domain plays a pivotal role in mediating cellular protection. In addition, with the exception of NAIP, all known IAP family members also contain a RING domain in their C terminus, defined by seven cysteine residues and one histidine residue that together coordinate two zinc atoms (36, 37). The RING domain confers E3 ubiquitin ligase activity and has been suggested to play a role in apoptosis regulation by directing the ubiquitination of target proteins for degradation by the proteasome (38–40). The RING domain is not essential for apoptosis inhibition by human IAP family members, which suggests that the BIR domain is sufficient to protect cells from apoptosis (41–43).

The genes that control PCD are functionally conserved across wide evolutionary distances (44–46). For example, homologues of the mammalian Bax-inducible cell death inhibitor BI-1 have been identified in several plants, including *Arabidopsis*, rice, tobacco, and barley (47–50). In addition, animal apoptotic regulators, such as human Bcl-2 and Bcl-xl as well as nematode CED-9, can either induce or suppress cell death in transgenic plants (51–53). In plants, PCD occurs during developmental processes, such as flower development, embryogenesis, seed germination, and vessel and trachea formation. Of note, PCD is crucial for a plant defense response termed hypersensitive response (HR), which serves to restrict the spread of pathogens through the process of PCD (54, 55). Studies in plant systems have shown that the biochemical and morphological hallmarks of apoptosis, such as cytoplasmic shrinkage, nuclear condensation, and DNA laddering, are similar in animal and plant cells (56–58). The cytosolic caspase-mediated apoptotic pathway is well defined in animal cells but has yet to be demonstrated in plant cells. However, evidence from recent studies has suggested that there are some similarities between plant apoptosis and caspase-mediated apoptosis in animal cells, with the exception of the presence of IAP-like proteins. For example, in tobacco cells, caspase-1-like proteases participate in HR, and the presence and subcellular localization of caspase-3-like proteases in barley has been reported (59–62).

In the current study, we identified and characterized a novel *Arabidopsis* gene, *AtILP* (for *Arabidopsis thaliana* IAP-like protein), which encodes a RING finger protein with homology to mammal IAPs. The expression of *AtILP* efficiently suppressed apoptosis induced by TNF-α/ActD and the fungal toxin fumonisin B1 (FB1) by blocking the activation of caspases in HeLa cells. Interestingly, despite lacking a BIR domain, an N-terminal fragment of AtILP conferred anti-apoptotic activity in *Arabidopsis*. Overexpression of the N-terminal domain of *AtILP* resulted in the suppression of FB1-induced cell death and attenuated cell death caused by the bacterial effector AvrRpt2. These results suggested that AtILP may act as a negative regulator of PCD in *Arabidopsis*.

EXPERIMENTAL PROCEDURES

Plasmid Construction—Plasmids encoding fragments of *AtILP* (including full-length *AtILP*; fragments a (residues 1–250), b (residues 1–150), c (residues 151–304), and d (residues 251–304); the N-terminal domain (residues 1–150); and the C-terminal domain (residues 151–304)) were created by one-step polymerase chain reaction (PCR) using a plasmid encoding full-length *AtILP* as the template. The sequences of the primers were as follows: 5′-GGATCCATGGCTGTTGAAGCTCATCACATG-3′ (for full-length *AtILP*, fragments a and b, and the N-terminal domain), 5′-GGATCCATGTCTGCGGTTCAAAAC-3′ (for fragment c and the C-terminal domain), and 5′-GGATCCATGGGTGGTTGTAAACGG-3′ (for fragment d) as the forward primers; 5′-CTCGAGTCAAGAAGACATGTTAACAT-3′ (full-length *AtILP*, fragments c and d, and the C-terminal domain), 5′-CTCGAGTCAAACCGCCGTTACCGGTT-3′ (fragment a), and 5′-CTCGAGTCACGCTAACATCCGCGTTTGCGT-3′ (fragment b and the N-terminal domain) as the reverse primers. Amplified full-length *AtILP* and fragments a, b, c, and d were digested with BamHI and XhoI and then subcloned into pcDNA3.1. Full-length *AtILP* and the N-terminal and C-terminal domain fragments were digested with BamHI and XhoI and then subcloned into pBI121 for expression in *Escherichia coli*.

Cell Culture and Cell Viability Assay—Human cervical epitheloid carcinoma (HeLa) cells were purchased from American Type Culture Collection (ATCC). HeLa cells were cultured in Dulbecco's modified Eagle's medium (DMEM; Invitrogen) supplemented with 10% heat-inactivated fetal bovine serum (FBS; Invitrogen), 2 mM L-glutamine, 100 units/ml penicillin, and 100 units/ml streptomycin in a humidified CO_2 incubator. Cells were transfected with the indicated expression vectors using Lipofectamine (63). Stable transfectants were selected in the presence of G418 (800 μg/ml).

Cell viability was determined by the crystal violet staining method. Briefly, HeLa cells plated in a 12-well dish were exposed to TNF-α (100 ng/ml)/ActD (100 ng/ml). Cells were stained with a solution of 0.5% crystal violet in 30% ethanol and 3% formaldehyde for 10 min at room temperature, after which the plates were washed three times with tap water. After drying, cells were lysed in 1% SDS, and dye uptake was measured at 550 nm using a 96-well plate reader. Cell viability was calculated as dye intensity relative to untreated samples.

DEVDase Activity Assay—Cell pellets were washed with ice-cold PBS and then resuspended in 100 mM HEPES buffer (pH 7.4) containing protease inhibitors (5 mg/ml aprotinin and pepstatin, 10 mg/ml leupeptin, and 0.5 mM phenylmethylsulfonyl fluoride). The cell suspension was lysed by three freeze-thaw cycles, and then the cytosolic fraction was obtained by centrifugation at 100,000 $\times$ *g* for 1 h at 4 °C. DEVDase activity was evaluated by measuring proteolytic cleavage of the chromogenic substrate Ac-DEVD-*p*NA, which serves as a substrate for

caspase-3-like proteases. Briefly, cell lysate (40 μg of protein) was mixed with 150 μl of reaction buffer containing Ac-DEVD-*p*NA (240 μM) in a 96-well plate. The reaction mixture was incubated at 37 °C for 90 min. The increase in enzymatically released *p*NA was measured every 15 min by absorbance at 405 nm; DEVDase activity was calculated from initial velocity.

For measuring DEVDase activity assay in plants, leaves were ground and homogenized in caspase extraction buffer (50 mM HEPES (pH 7.5), 1 mM EDTA, 1 mM DTT, 1% BSA, 1 mM PMSF, 20% glycerol). Samples were mixed with 50 μl of caspase assay buffer (caspase extraction buffer containing 150 μM Ac-DEVD-*p*NA) and then incubated at 37 °C for 1 h. The increase in enzymatically released *p*NA was measured every 15 min by absorbance at 405 nm; DEVDase activity was calculated from the initial velocity.

Plants—A. thaliana seedlings were germinated on MS medium containing 2% sucrose and 0.6% Phytagel and maintained in a temperature- and light-controlled growth chamber. *Arabidopsis* seedlings were grown for 14 days before being transferred to fresh MS plates or to fresh MS plates supplemented with FB1.

For the DNA fragmentation assay, 10 μg of genomic DNA was separated by electrophoresis on a 0.8% agarose, 0.6% MetaPhor-agarose gel and then transferred to a Hybond membrane. As a probe, 50 ng of total genomic *Arabidopsis* DNA was labeled using a commercially available random labeling kit. Following hybridization, the membrane was washed with 0.1× SSC, 0.1% SDS at 65 °C for 2 h.

Bacteria—Bacterial strains were grown at 28 °C on KB medium containing the appropriate antibiotics for selection. For assessing ion leakage and to score HR phenotype, plants were infiltrated with 10^7 cfu/ml (A_{600} = 0.2) of *Pseudomonas syringae* pv. *phaseolicola* (Pph) strain NPS3121 using a needleless 1-ml syringe (see Table 1 and Fig. 6). Pph strain NPS3121 harboring *AvrRpt2* was used for the ion leakage and cell death assay. For ion leakage measurements, eight leaf discs (8 mm in diameter) were removed immediately following infiltration (t = 0) and allowed to float in 40 ml of water. After 30 min, the wash water was replaced with 10 ml of fresh water, and then conductance over time was measured using a Fisher brand conductivity meter.

For growth experiments using *P. syringae* pv. *maculicola* (Pma) strain M6CΔE (64) harboring empty vector (pVSP61) or its derivative encoding *AvrRpt2* (Fig. 7), the leaves of 5-week-old plants were inoculated with bacterial suspensions in 10 mM $MgCl_2$ using a needleless 1-ml syringe. After the indicated periods of time, three leaf discs for each sample were ground in 10 mM $MgCl_2$ and then serially diluted and plated to determine bacterial number.

Subcellular Localization of AtILP Fusion Protein—PCR was used to generate a cDNA fragment encoding full-length *AtILP*. The cDNA fragment was digested with XbaI and BamHI and then ligated in-frame with soluble modified green fluorescent protein (smGFP) to create *AtILP*::*smGFP*. The *AtILP*::*smGFP* fusion construct was introduced into *Arabidopsis* protoplasts using polyethylene glycol-mediated transformation. The expression of red fluorescent protein fused to a nuclear localization signal (RFP::NLS) was used as a positive control for nuclear localization. Transformed protoplasts were incubated at 22 °C in the dark. Expression of fusion protein was observed 2 days after transformation by fluorescence microscopy (Olympus AX70) using standard FITC and rhodamine filters.

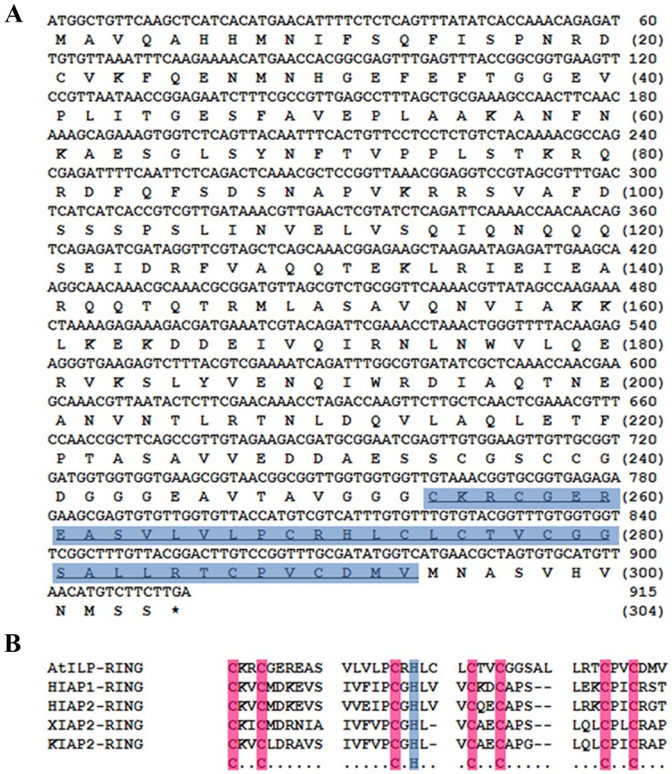

FIGURE 1. **Nucleotide and deduced amino acid sequence of *AtILP* and comparison of its RING domain with other IAPs.** *A*, amino acid residues are numbered at the *right*, and the putative RING domain is shown in *blue*. *B*, the RING domains aligned for comparison are from *A. thaliana* (*AtILP*) and *H. sapiens* (*HIAP1*, *HIAP2*, *XIAP*, and *KIAP*). Sequences were obtained from the SwissProt data base; conserved cysteine and histidine residues are indicated in *pink* and *blue*, respectively.

RESULTS

Identification of an Apoptosis Inhibitor in Arabidopsis and Demonstration of Anti-apoptotic Activity in Animal Cells—Some aspects of the signaling mechanisms that control apoptosis, including IAP family members, are functionally conserved across wide evolutionary distances. HIAP1 and HIAP2 are functional anti-apoptotic proteins in *Homo sapiens* (65–67). To determine whether higher plants carry HIAP-like proteins, homology searches against the *Arabidopsis* genome sequence database were performed using the sequences of HIAP1 and -2 as the queries. The searches yielded one gene, At4g19700, encoding a putative protein with significant similarity to other IAPs. In particular, the protein contained a RING domain in its C terminus. This protein was named AtILP, for *A. thaliana* IAP-like protein. The full-length *AtILP* cDNA was isolated from an *Arabidopsis* cDNA library. It consisted of 915 nucleotides encoding a putative open reading frame of 305 amino acids (Fig. 1*A*). Amino acid sequence alignment of the RING domain of *AtILP* with human *HIAP1*, *HIAP2*, *XIAP*, and *KIAP* showed that *AtILP* encodes a perfect C-terminal C3HC4 signature (Fig. 1*B*). Aside from the highly conserved RING domain, AtILP did not appear to encode any other known conserved domains.

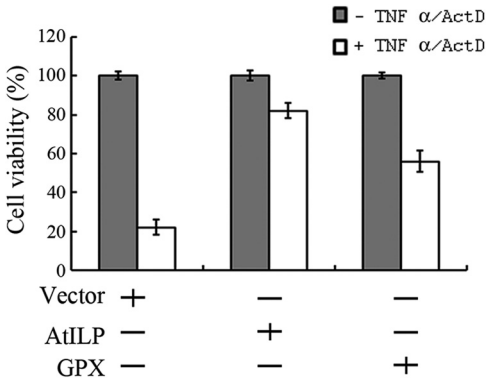

FIGURE 2. **Inhibitory effect of AtILP on TNF-α/ActD-induced apoptosis.** HeLa cells were transiently co-transfected with empty vector or with expression vectors for AtILP or GPx as a positive control. The percentage of cell viability was calculated based on dye intensity relative to that of the untreated apoptosis inducer sample. *Column A*, vector alone as a negative control; *column B*, AtILP; *column C*, GPx as a positive control. Data represent three independent experiments. *Error bars*, S.D.

IAP proteins are characterized by the presence of one or more BIR domains, a structurally distinct, zinc finger fold domain composed of ~70 amino acid residues. It is widely acknowledged that the BIR domain is essential for the anti-apoptotic properties of the IAP proteins in animal systems. To determine whether AtILP possessed anti-apoptotic activity, despite not having a BIR domain, HeLa cells were transfected with expression vectors for *AtILP* or *Gpx* or empty vector (pcDNA) as a control using Lipofectamine (63), and the response to TNF-α/ActD-induced cell death was analyzed. Gpx was used as a positive control for apoptosis inhibition (68, 69). As shown in Fig. 2, TNF-α/ActD-induced cell death was considerably reduced in cells expressing *AtILP*, even more so than in *GPx*-expressing cells. The viability of *AtILP*-expressing cells exceeded 85%, whereas that of *GPx*-expressing cells was ~55%. These results indicated that *AtILP* is a RING finger protein with structural and possibly functional homology to human IAPs and that a gene involved in apoptosis inhibition in plants functions in a similar manner in an animal system.

The N-terminal Domain of AtILP Blocks TNF-α/ActD-induced Caspase Activation—To define the molecular determinants of AtILP anti-apoptotic activity, four different AtILP protein fragments were constructed (Fig. 3*B*). HeLa cells were transfected with expression vectors for full-length AtILP or one of the AtILP fragments (fragment a, b, c, or d), and then anti-apoptotic activity was measured. Because AtILP did not have a BIR domain, and computer-based sequence homology searches revealed no other similarities with other IAP proteins, we initially expected that the functional domain would map to the C-terminal RING domain. As shown in Fig. 3*A*, cells transfected with empty vector or fragments c and d underwent cell death in response to TNF-α/ActD. In contrast, transfection expression vectors for full-length AtIPL, fragment a, or fragment b significantly reduced TNF-α/ActD-induced apoptosis. Fragments a and b retained ~75% of the inhibitory activity of the full-length protein, whereas the anti-apoptotic activity of fragments c and d, which contained the C-terminal RING domain, were comparable with control conditions (Fig. 3*B*). The various AtILP fragments are depicted schematically in Fig.

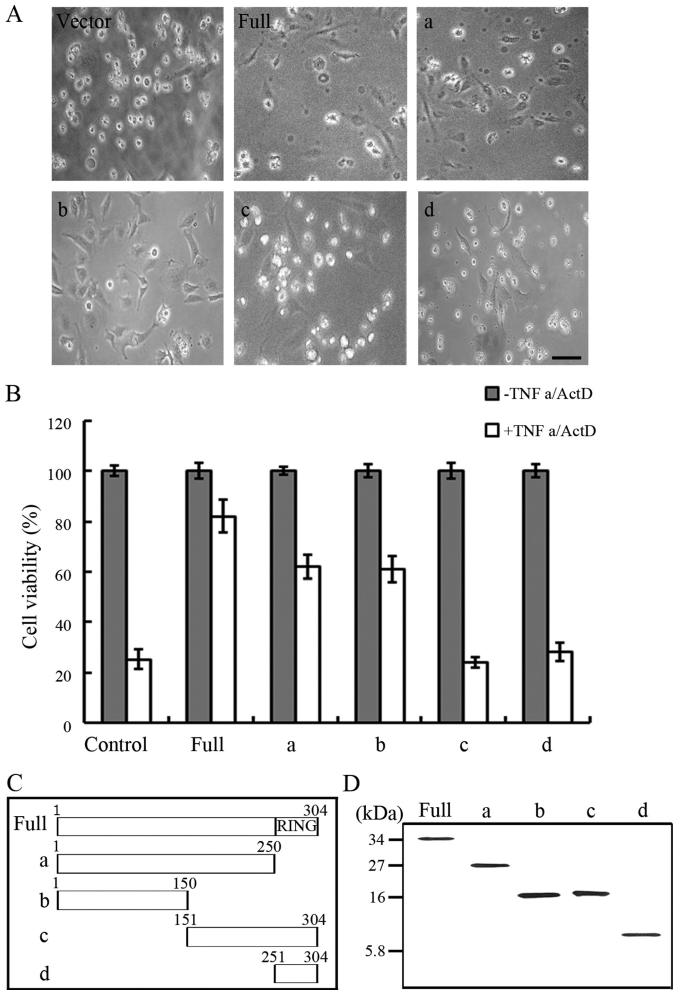

FIGURE 3. **The N-terminal region of AtILP suppresses TNF-α/ActD-induced apoptosis.** *A*, morphological changes of apoptotic cells treated with TNF-α/ActD. *Scale bar*, 10 μm. *a–d*, fragments of AtILP. *B*, cells were treated as for Fig. 2, except that HeLa cells were transiently co-transfected with expression vectors for full-length AtILP or the indicated fragment of AtILP. *C*, schematic representation of full-length *AtILP* and the truncation mutants. *D*, total protein extracts from HeLa cells were separated by 13% SDS-PAGE, and AtILP was detected by immunoblot analysis using anti-AtILP antibodies. *Error bars*, S.D.

3*B*. Full-length AtILP and the AtILP fragments were all stably expressed in HeLa cells (Fig. 3*C*). These results indicated that fragment b, which contained the N-terminal 150 amino acid residues of AtILP, contains the main determinant(s) of anti-apoptotic activity.

Because caspases are critical mediators of apoptosis, we next examined whether caspase inactivation played a role in the anti-apoptotic activity of AtILP. DEVDase activity was evaluated by measuring the proteolytic cleavage of a chromogenic substrate, Ac-DEVD-*p*NA, which serves as a substrate of caspase-3-like proteases. As seen in Fig. 4, the inhibitory effects of full-length AtILP and each of the AtILP fragments on DEVDase inactivation correlated with the results of the cell viability assay. These data clearly suggested that the activity of AtILP in inhibiting cell death is mediated by the N-terminal domain through the suppression of caspase activation (Fig. 4).

The N-terminal Domain of AtILP Confers Resistance to FB1-induced Apoptosis in Arabidopsis—To evaluate the role of AtILP in apoptosis inhibition in plants, transgenic *Arabidopsis*

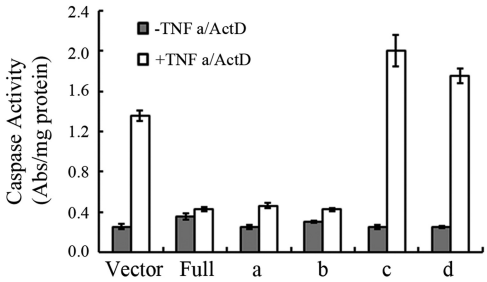

FIGURE 4. **AtILP suppresses TNF-α/ActD-induced apoptosis by blocking caspase activation.** Protein extracts from transfected HeLa cells treated with TNF-α/ActD were incubated with peptide substrate (Ac-DEVD-*p*NA) in caspase assay buffer. Fluorescence was measured at 405 nm. Data represent the results of one of three independent replicates. *a–d*, fragments of AtILP. *Error bars*, S.D.

lines that constitutively expressed full-length *AtILP* or the N-terminal (amino acids 1–150) or C-terminal (amino acids 151–304) domain of *AtILP* under the control of the cauliflower mosaic virus (CaMV) 35S promoter were generated. Several transgenic plants that exhibited high levels of expression of full-length, N-terminal, or C-terminal AtILP were selected for further analysis (supplemental Fig. 1). The N-terminal and C-terminal domains consisted of 150 and 154 amino acids, respectively. A striking example of plant apoptosis, HR is a cell death program triggered in host cells at or around the site of pathogen infection, resulting in cellular collapse and the formation of necrotic lesions (70). Because it is well known that the fungal toxin FB1 induces HR in plants (56, 71, 72), we examined the effect of the overexpression of full-length AtILP or the N- or C-terminal domain on FB1-induced HR in *Arabidopsis*. Wild-type *Arabidopsis* ecotype Col-0 and transgenic *Arabidopsis* plants were grown for 2 weeks on MS agar medium, transferred to MS medium containing 3 μM FB1, and then observed for morphological changes 4 days after transfer. As shown in Fig. 5*A*, the leaves of wild-type and transgenic plants harboring the C-terminal fragment of AtILP were completely macerated, and death lesions were readily apparent. In contrast, transgenic plants expressing full-length *AtILP* or the N-terminal domain exhibited some lesions in the upper leaves but overall were highly resistant to FB1-induced cell death compared with wild-type and C-terminal domain transgenic plants.

Caspase-like activity and a role for caspase-like proteases in HR have been reported in plants, and HR can be prevented through the inhibition of caspase-like proteases (59, 73). To determine whether the anti-apoptotic activity of AtILP in plants exposed to FB1 was mediated by caspase-like protease inactivation, as was seen in HeLa cells (Fig. 4), protein extracts from wild-type and transgenic plants were prepared. As seen in Fig. 5*B*, caspase inactivation correlated with the ability of full-length AtILP and the N- and C-terminal domains to suppress FB1-induced apoptosis. Treatment with FB1 induced the activation of caspase-like proteases in wild-type and C-terminal domain transgenic plants. In contrast, the overexpression of full-length AtILP or the N-terminal domain effectively suppressed caspase-like protease activation (Fig. 5*B*). These results suggested that the isolated N-terminal domain of AtILP can prevent plant cell death by suppressing caspase-like protease activation.

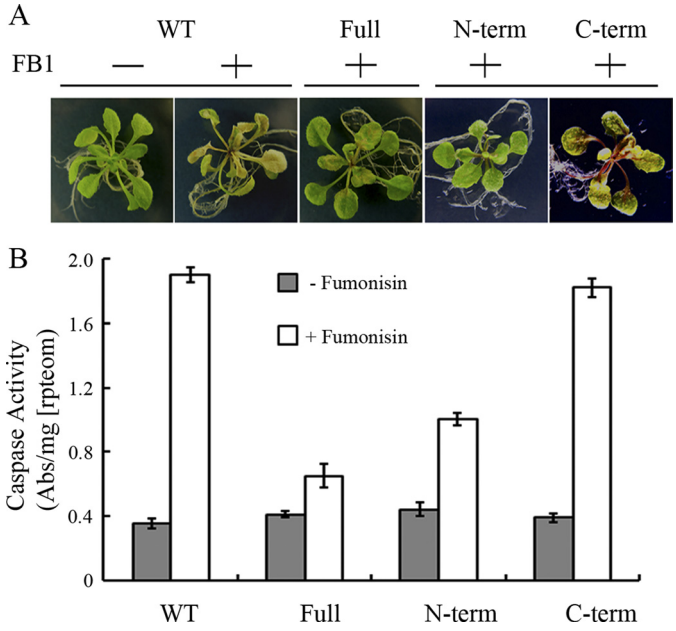

FIGURE 5. **Overexpression of *AtILP* confers resistance against HR induced by FB1 treatment.** *A*, 2-week-old wild-type and transgenic *Arabidopsis* seedlings were transferred to MS plates (−*FB1*) or MS plates supplemented with 3 μM FB1. Seedlings were photographed 5 days after transfer. Wild-type and transgenic plants grown on MS plates without FB1 were indistinguishable. *B*, protein extracts from transgenic plant lines grown on MS plates with or without 3 μM FB1 were incubated with peptide substrate (Ac-DEVD-*p*NA) in caspase assay buffer. Fluorescence was measured at 405 nm. Data represent the results of one of three independent replicates. *Error bars*, S.D.

Effect of AtILP on the Interaction between Arabidopsis and the Bacterial Pathogen P. syringae—It was next examined whether the expression of *AtILP* altered effector protein-induced HR and the associated cell death. Gram-negative plant pathogenic bacteria secrete a complex set of effectors, making it difficult to detect changes in HR induced by a single effector protein. To overcome this limitation, a strain of Gram-negative phytopathogenic bacteria, Pph strain NPS3121, was used that expressed the avirulent gene *AvrRpt2*. Using this strain, it was possible to measure HR and electrolyte leakage in response to an avirulent bacterial pathogen. The leaves of 6-week-old *Arabidopsis* plants (wild-type and *AtILP* transgenic lines) were infiltrated with Pph strain NPS3121 expressing *AvrRpt2* (Pph (AvrRpt2)) at a dose of 10^7 cfu/ml (see "Experimental Procedures"). Within 16 h, most wild-type and transgenic plants overexpressing the C-terminal domain of *AtILP* exhibited confluent tissue collapse at the site of pathogen infiltration, which is a characteristic feature of HR-associated cell death. However, most of the leaves of the transgenic plants overexpressing full-length *AtILP* or the N-terminal domain did not show serious signs of HR, although a small percentage developed a weak HR at 16 h. This weak HR in full-length *AtILP* and N-terminal domain transgenic plants was restricted to a small area surrounding the point of infiltration and was not confluent. Confluent tissue collapse was observed in most of the inoculated leaves of the transgenic plants by 20 h postinoculation (Table 1).

Electrolyte leakage due to membrane damage as a result of plant-pathogen interaction is a characteristic and quantitative feature of HR-associated cell death (74). To determine whether

TABLE 1

Overexpression of full-length *AtILP* or the N-terminal region attenuates the hypersensitive response induced by *P. syringae* pv. *phaseolicola* NPS3121 expressing *AvrRpt2*. Shown are numbers of at least half-collapsed leaves of a total of 20 infiltrated leaves

Plant	8 h	16 h	24 h
Col-0	2/20	18/20	20/20
Full-length *AtILP*-expressing *Arabidopsis* line 1	0/20	8/20	17/20
Full-length *AtILP*-expressing *Arabidopsis* line 2	0/20	9/20	18/20
N terminus *AtILP*-expressing *Arabidopsis* line 1	0/20	7/20	17/20
N terminus *AtILP*-expressing *Arabidopsis* line 2	0/20	8/20	18/20
C terminus *AtILP*-expressing *Arabidopsis* line 1	1/20	17/20	20/20
C terminus *AtILP*-expressing *Arabidopsis* line 2	2/20	19/20	20/20

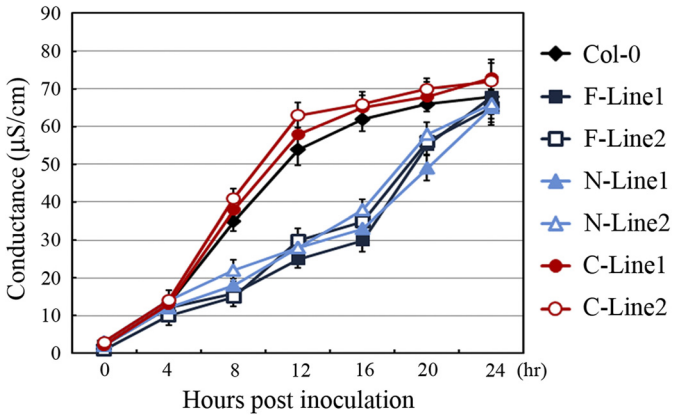

FIGURE 6. **Overexpression of full-length *AtILP* or the N-terminal domain suppresses electrolyte leakage.** Wild-type or transgenic *Arabidopsis* overexpressing *AtILP* or *AtILP* domains were infiltrated with *P. syringae* pv. *phaseolicola* NPS3121 expressing *AvrRpt2* at a dose of 10^7 cfu/ml. Leaf discs were removed for conductivity measurements over time. The results represent mean microsiemens ± S.D. from one of three independent replicates.

the attenuation of HR was related to membrane damage, electrolyte leakage in wild-type and *AtILP* transgenic plants was measured after Pph (AvrRpt2) infiltration (10^7 cfu/ml). Leaves from wild-type and transgenic plants overexpressing the C-terminal domain of *AtILP* reached close to maximal conductivity 12–16 h postinoculation. Transgenic plants overexpressing full-length *AtILP* or the N-terminal domain exhibited a similar pattern, but the magnitude of the response was significantly lower, and maximal conductivity was reached later compared with wild-type or C-terminal domain transgenic plants (Fig. 6). However, a difference in conductivity was not observed when plants were treated with virulent bacterial pathogen Pph (data not shown). These results indicated that the overexpression of the N-terminal domain of *AtILP* significantly impairs HR-associated cell death elicited by an avirulent bacterial pathogen.

To further explore the role of *AtILP* in plant defense response, the effect of attenuated cell death on bacterial growth was assessed using the bacterial pathogen Pma strain M6CΔE. Disease phenotype was assessed following the inoculation of this virulent strain of *P. syringae* (Pma strain M6CΔE) into wild-type and *AtILP* transgenic lines. All of the plants (transgenic and wild type) exhibited visible chlorosis 3–4 days after inoculation, which progressed over time on the infected leaves. The plant lines were indistinguishable in terms of the severity of chlorosis (data not shown). In addition, there were no differences in bacterial titer among wild-type and *AtILP* transgenic lines (Fig. 7*A*). These results indicated that the overexpression of *AtILP* does not alter the defense response to infection with virulent Pma strain M6CΔE.

To determine whether *AtILP*-mediated HR attenuation affected the growth of an avirulent strain of Pma, strain M6CΔE carrying the avirulence gene *AvrRpt2* was used as the inoculum. In this case, the overexpression of full-length *AtILP* or the N-terminal domain resulted in a 30–40-fold increase in bacterial growth, which indicated that the overexpression of *AtILP* decreases resistance to avirulent Pma strain M6CΔE (Fig. 7*B*).

AtILP Localizes to the Nucleus and Blocks DNA Fragmentation—Genomic DNA fragmentation during the process of PCD occurs as a result of the activation of cell death-specific endonucleases that cleave nuclear DNA into oligonucleosomal units. Genomic DNA was extracted from wild-type and transgenic plants treated with or without 3 μM FB1. As shown in Fig. 8*A*, in transgenic plants harboring full-length *AtILP* or the N-terminal domain, FB1-induced DNA fragmentation was inhibited. Given that DNA fragmentation is a hallmark of apoptosis, these results confirmed that *AtILP* blocks apoptosis in plants and that the N-terminal domain of *AtILP* is important for this anti-apoptotic activity.

To confirm that AtILP was present in the nucleus to mediate genomic DNA fragmentation, the subcellular localization of AtILP *in vivo* was analyzed in *Arabidopsis*. A C-terminal smGFP fusion protein of AtILP was generated and expressed in *Arabidopsis* protoplasts. Fluorescence microscopy revealed that AtILP localized to the nucleus (Fig. 8*B*), and there was some overlap with the control protein, RFP::NLS. These results indicated that AtILP is targeted exclusively to the nucleus in plant cells.

DISCUSSION

A number of genes that regulate PCD, both positively and negatively, have been identified; however, the mechanisms that control PCD in plants remain largely unknown. In the current study, a novel *Arabidopsis* RING finger protein, AtILP, was identified and shown to be a negative regulator of PCD in *Arabidopsis*. Overexpression of AtILP suppressed effector protein- and FB1-induced cell death. In addition, AtILP blocked TNF-/ActD-induced cell death via the suppression of caspase activation in HeLa cells, suggesting that the function of AtILP in inhibiting cell death is preserved across species.

To determine the structural basis for the inhibition of apoptosis by AtILP, the effects of various fragments of AtILP on caspase activity *in vitro* and on apoptosis suppression in HeLa cells were analyzed. The RING domain of AtILP failed to inhibit the activity of caspase-3, whereas an N-terminal fragment that had no homology to any known BIR domain potently inhibited the activity of caspase-3 *in vitro* and blocked TNF-α/ActD-induced apoptosis (Figs. 3 and 4). Amino acid sequence alignment with other IAP proteins indicated that AtILP lacks homology to known BIR domains. The secondary structure of AtILP was investigated, and it was found that AtILP and human IAPs share a common motif consisting of three consecutive β strands, an α helix, a β strand, and an α helix (supplemental Fig. 2). One possibility is that these common structural motifs determine the caspase-inhibitory activity of AtILP.

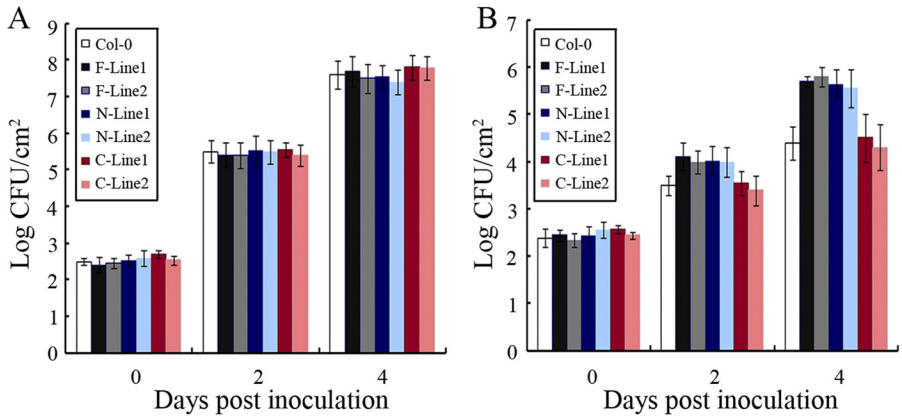

FIGURE 7. **Growth of Pma M6CΔE carrying empty vector or expressing *AvrRpt2* in wild-type and transgenic *Arabidopsis*.** Plants were infiltrated with Pma M6CΔE carrying empty vector (*A*) or expressing *AvrRpt2* (*B*) at a dose of 10^4 cfu/ml. Bacterial titers in leaves were determined at the indicated time points. The results represent mean cfu/cm^2 ± S.D. (*error bars*) from one of four independent replicates.

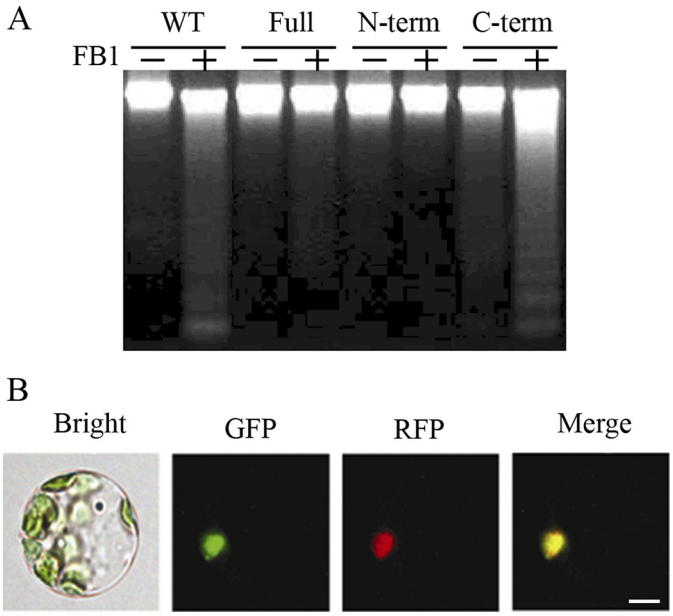

FIGURE 8. **Inhibition of DNA fragmentation by AtILP and subcellular localization of AtILP in *Arabidopsis* protoplasts.** *A*, wild-type and transgenic plants were grown on an MS plate with or without 3 μM FB1. Genomic DNA was isolated, separated by electrophoresis, and then visualized by staining with ethidium bromide. *B*, 10-day-old *Arabidopsis* protoplasts were co-transformed with 10 μg of *AtILP*::*smGFP* and *RFP*::*NLS* expression constructs. RFP::NLS was used as a control for nuclear localization. *Images* labeled *Bright*, *GFP*, and *RFP* were obtained by fluorescence microscopy. Co-localization of GFP and RFP (*Merge*) appears as *yellow*. *Scale bar*, 10 μm.

Based on amino acid sequences analysis, AtILP belongs to the family of RING proteins, members of which have diverse biological functions in plants (75). AtILP contained a well conserved RING domain at its C terminus. Overexpression of *AtILP* in plants resulted in the reduction of cell death in response to an avirulent bacterial pathogen and to low doses of FB1. Most RING finger proteins have enzymatic activities that catalyze reactions within the ubiquitination/26S proteasome protein degradation system (75, 76). Many IAP proteins exhibit E3 ubiquitin ligase activity, and the RING domain is critical for biological activity and regulation of PCD (77–80). In fact, *Arabidopsis* RING1, which demonstrates E3 ubiquitin ligase activity *in vitro*, has been implicated in cell death (76). The biochemical activity and putative function of another RING domain protein in *Arabidopsis*, AtHAL1, remain to be elucidated.

Transgenic *Arabidopsis* lines that overexpressed *AtILP* demonstrated anti-apoptotic activity when challenged with the fungal toxin FB1. This suppression of cell death was accompanied by the inhibition of caspase activation and DNA fragmentation. The anti-apoptotic activity of AtILP mapped to the N-terminal domain and correlated with the results of similar experiments in HeLa cells. To investigate the role of AtILP in cell death inhibition, T-DNA insertion mutagenesis was carried out, and several *AtILP* knock-out plant lines were identified and characterized. Mutation of *AtILP* did not result in any phenotypic differences in terms of germination, flowering, and growth rate as compared with wild-type plants. In addition, plant responses to FB1 and *P. syringae* pv. *tomato* DC3000 expressing *AvrRpt2* were indistinguishable from wild-type *Arabidopsis*, indicating that there may be other as yet unidentified genes in *Arabidopsis* that can compensate for the loss of the cell death inhibition activity of *AtILP* (data not shown).

Gram-negative plant pathogenic bacteria secrete a complex set of type III effectors directly into host cells via the type III secretion system. For example, the wild-type Pto strain delivers at least 33, and perhaps as many as 50, type III effectors (81, 82). Thus, HR in response to bacterial strain Pto is a cumulative effect of multiple effector proteins. As a result, it is almost impossible to detect HR induced by a single effector protein. In the current study, Gram-negative phytopathogenic bacteria Pph strain NPS3121 expressing *AvrRpt2* was used. Pph does not trigger HR, which can obscure other defense responses. Pph is a model pathogen that causes halo blight in bean but not in *Arabidopsis* (83). Thus, the use of this pathogen enabled us to measure the effect of AvrRpt2 on HR and electrolyte leakage.

In many cases, PCD and disease resistance are intricately linked in higher plants (84). During incompatible interactions between plants and bacterial pathogens, HR-associated cell death often triggers the development of plant disease resistance, resulting in the halting of pathogen growth in plant tissues. Cell death, however, can be uncoupled from the resistance response. For example, the *Arabidopsis* mutant *dnd1* (defense no death) is resistant to *Pst* without HR-associated cell death (85). In the current study, overexpression of *AtILP* caused a

decrease in the stress response to an avirulent strain of Pph that resulted in reduced HR cell death. In addition, transgenic *Arabidopsis* lines overexpressing *AtILP* supported higher levels of bacterial growth compared with wild-type plants after inoculation with Pma M6CΔE harboring *AvrRpt2*. These results indicate that AtILP has distinct functions in regulating PCD and disease resistance (*i.e.* a negative role in *AvrRpt2*-induced PCD and a positive role in *RPS2*-mediated resistance). Furthermore, neither the overexpression (Fig. 7*A*) nor mutation of *AtILP* (data not shown) affected the response of plants to a virulent strain (Pma M6CΔE). Therefore, reduced PCD in *AtILP* plants is likely to be unrelated to the defense response to virulent pathogens.

REFERENCES

1. Kimchi, A. (2007) *Cytokine Growth Factor Rev.* **18,** 435–440
2. Steller, H. (1995) *Science* **267,** 1445–1499
3. Vaux, D. L., and Korsmeyer, S. J. (1999) *Cell* **96,** 245–254
4. Jacobson, M. D., Weil, M., and Raff, M. C. (1997) *Cell* **88,** 347–354
5. Peter, M. E. (2011) *Nature* **471,** 310–312
6. Burguillos, M. A., Hajji, N., Englund, E., Persson, A., Cenci, A. M., Machado, A., Cano, J., Joseph, B., and Venero, J. L. (2011) *Neurobiol. Dis.* **41,** 177–188
7. Tripathy, M. K., Ahmed, Z., Ladha, J. S., and Mitra, D. (2010) *Apoptosis* **15,** 1453–1460
8. Thornberry, N. A., and Lazebnik, Y. (1998) *Science* **281,** 1312–1316
9. Hengartner, M. O. (1998) *Nature* **391,** 441–442
10. Behjati, R., Kawai, K., Inadome, Y., Kano, J., Akaza, H., and Noguchi, M. (2011) *Cancer Sci.* **102,** 267–274
11. Malladi, S., Challa-Malladi, M., Fearnhead, H. O., and Bratton, S. B. (2009) *EMBO J.* **28,** 1916–1925
12. Ali, S., Nguyen, D. Q., Falk, W., and Martin, M. U. (2010) *Biochem. Biophys. Res. Commun.* **391,** 1512–1516
13. Hörnle, M., Peters, N., Thayaparasingham, B., Vörsmann, H., Kashkar, H., and Kulms, D. (2011) *Oncogene* **30,** 575–587
14. Thornberry, N. A. (1997) *Br. Med. Bull.* **53,** 478–490
15. Conus, S., Perozzo, R., Reinheckel, T., Peters, C., Scapozza, L., Yousefi, S., and Simon, H. U. (2008) *J. Exp. Med.* **205,** 685–698
16. Pereira, W. F., Guillermo, L. V., Ribeiro-Gomes, F. L., and Lopes, M. F. (2008) *An. Acad. Bras. Cienc.* **80,** 129–136
17. Muzio, M., Stockwell, B. R., Stennicke, H. R., Salvesen, G. S., and Dixit, V. M. (1998) *J. Biol. Chem.* **273,** 2926–2930
18. Yu, D., Nagamura, Y., Shimazu, S., Naito, J., Kaji, H., Wada, S., Honda, M., Xue, L., and Tsukada, T. (2010) *Endocr. J.* **57,** 825–832
19. MacNeill, A. L., Moldawer, L. L., and Moyer, R. W. (2009) *Virology* **384,** 151–160
20. Bump, N. J., Hackett, M., Hugunin, M., Seshagiri, S., Brady, K., Chen, P., Ferenz, C., Franklin, S., Ghayur, T., and Li, P. (1995) *Science* **269,** 1885–1888
21. Xue, D., and Horvitz, H. R. (1995) *Nature* **377,** 248–251
22. Zhou, Q., Snipas, S., Orth, K., Muzio, M., Dixit, V. M., and Salvesen, G. S. (1997) *J. Biol. Chem.* **272,** 7797–7800
23. Sung, J. H., Zhao, H., Roy, M., Sapolsky, R. M., and Steinberg, G. K. (2007) *Neuroscience* **149,** 804–812
24. Clem, R. J., and Miller, L. K. (1994) *Mol. Cell. Biol.* **14,** 5212–5222
25. Crook, N. E., Clem, R. J., and Miller, L. K. (1993) *J. Virol.* **67,** 2168–2174
26. Roy, N., Mahadevan, M. S., McLean, M., Shutler, G., Yaraghi, Z., Farahani, R., Baird, S., Besner-Johnston, A., Lefebvre, C., and Kang, X. (1995) *Cell* **80,** 167–178
27. Ambrosini, G., Adida, C., and Altieri, D. C. (1997) *Nat. Med.* **3,** 917–921
28. Duckett, C. S., Nava, V. E., Gedrich, R. W., Clem, R. J., Van Dongen, J. L., Gilfillan, M. C., Shiels, H., Hardwick, J. M., and Thompson, C. B. (1996) *EMBO J.* **15,** 2685–2694
29. Hay, B. A. (2000) *Cell Death Differ.* **7,** 1045–1056
30. Hay, B. A., Wassarman, D. A., and Rubin, G. M. (1995) *Cell* **83,** 1253–1262
31. Rothe, M., Pan, M. G., Henzel, W. J., Ayres, T. M., and Goeddel, D. V. (1995) *Cell* **83,** 1243–1252
32. Salvesen, G. S., and Duckett, C. S. (2002) *Nat. Rev. Mol. Cell Biol.* **3,** 401–410
33. Liston, P., Fong, W. G., and Korneluk, R. G. (2003) *Oncogene* **22,** 8568–8580
34. Jones, G., Jones, D., Zhou, L., Steller, H., and Chu, Y. (2000) *J. Biol. Chem.* **275,** 22157–22165
35. Vucic, D., Franklin, M. C., Wallweber, H. J., Das, K., Eckelman, B. P., Shin, H., Elliott, L. O., Kadkhodayan, S., Deshayes, K., Salvesen, G. S., and Fairbrother, W. J. (2005) *Biochem. J.* **385,** 11–20
36. Borden, K. L. (2000) *J. Mol. Biol.* **295,** 1103–1112
37. Wei, Y., Fan, T., and Yu, M. (2008) *Acta Biochim. Biophys. Sin.* **40,** 278–288
38. Ni, T., Li, W., and Zou, F. (2005) *IUBMB Life* **57,** 779–785
39. Vaux, D. L., and Silke, J. (2005) *Nat. Rev. Mol. Cell Biol.* **6,** 287–297
40. Morizane, Y., Honda, R., Fukami, K., and Yasuda, H. (2005) *J. Biochem.* **137,** 125–132
41. Xu, M., Okada, T., Sakai, H., Miyamoto, N., Yanagisawa, Y., MacKenzie, A. E., Hadano, S., and Ikeda, J. E. (2002) *Biochim. Biophys. Acta* **1574,** 35–50
42. Herman, M. D., Moche, M., Flodin, S., Welin, M., Trésaugues, L., Johansson, I., Nilsson, M., Nordlund, P., and Nyman, T. (2009) *Acta Crystallogr. Sect. F Struct. Biol. Cryst. Commun.* **65,** 1091–1096
43. Watihayati, M. S., Zabidi-Hussin, A. M., Tang, T. H., Matsuo, M., Nishio, H., and Zilfalil, B. A. (2007) *Pediatr. Int.* **49,** 11–14
44. Higashi, K., Takasawa, R., Yoshimori, A., Goh, T., Tanuma, S., and Kuchitsu, K. (2005) *Apoptosis* **10,** 471–480
45. Williams, B., and Dickman, M. (2008) *Mol. Plant Pathol.* **9,** 531–544
46. Boyce, M., Degterev, A., and Yuan, J. (2004) *Cell Death Differ.* **11,** 29–37
47. Lacomme, C., and Santa Cruz, S. (1999) *Proc. Natl. Acad. Sci. U.S.A.* **96,** 7956–7961
48. Watanabe, N., and Lam, E. (2006) *Plant J.* **45,** 884–894
49. Eichmann, R., Schultheiss, H., Kogel, K. H., and Hückelhoven, R. (2004) *Mol. Plant Microbe Interact.* **17,** 484–490
50. Matsumura, H., Nirasawa, S., Kiba, A., Urasaki, N., Saitoh, H., Ito, M., Kawai-Yamada, M., Uchimiya, H., and Terauchi, R. (2003) *Plant J.* **33,** 425–434
51. Dickman, M. B., Park, Y. K., Oltersdorf, T., Li, W., Clemente, T., and French, R. (2001) *Proc. Natl. Acad. Sci. U.S.A.* **98,** 6957–6962
52. Lincoln, J. E., Richael, C., Overduin, B., Smith, K., Bostock, R., and Gilchrist, D. G. (2002) *Proc. Natl. Acad. Sci. U.S.A.* **99,** 15217–15221
53. Xu, P., Rogers, S. J., and Roossinck, M. J. (2004) *Proc. Natl. Acad. Sci. U.S.A.* **101,** 15805–15810
54. Beers, E. P., and McDowell, J. M. (2001) *Curr. Opin. Plant Biol.* **4,** 561–567
55. Gechev, T. S., Van Breusegem, F., Stone, J. M., Denev, I., and Laloi, C. (2006) *BioEssays* **28,** 1091–1101
56. Basnayake, B. M., Li, D., Zhang, H., Li, G., Virk, N., and Song, F. (2011) *Plant Cell Rep.* **30,** 37–48
57. Solomon, M., Belenghi, B., Delledonne, M., Menachem, E., and Levine, A. (1999) *Plant Cell* **11,** 431–444
58. He, X., and Kermode, A. R. (2003) *Plant Mol. Biol.* **52,** 729–744
59. del Pozo, O., and Lam, E. (1998) *Curr. Biol.* **8,** 1129–1132
60. Korthout, H. A., Berecki, G., Bruin, W., van Duijn, B., and Wang, M. (2000) *FEBS Lett.* **475,** 139–144
61. Bonneau, L., Ge, Y., Drury, G. E., and Gallois, P. (2008) *J. Exp. Bot.* **59,** 491–499
62. Lam, E., and del Pozo, O. (2000) *Plant Mol. Biol.* **44,** 417–428
63. Kim, Y. M., Talanian, R. V., and Billiar, T. R. (1997) *J. Biol. Chem.* **272,** 31138–31148
64. Rohmer, L., Kjemtrup, S., Marchesini, P., and Dangl, J. L. (2003) *Mol. Microbiol.* **47,** 1545–1562
65. Leong, W. F., Tan, H. C., Ooi, E. E., Koh, D. R., and Chow, V. T. (2005) *Microbes Infect.* **7,** 248–259
66. Harvey, H. A. (1998) *Oncology* **12,** 32–35
67. LaCasse, E. C., Baird, S., Korneluk, R. G., and MacKenzie, A. E. (1998) *Oncogene* **17,** 3247–3259
68. Crack, P. J., Taylor, J. M., Flentjar, N. J., de Haan, J., Hertzog, P., Iannello, R. C., and Kola, I. (2001) *J. Neurochem.* **78,** 1389–1399

69. Mu, Y., Lv, S., Ren, X., Jin, G., Liu, J., Yan, G., Li, W., Shen, J., and Luo, G. (2003) *J. Photochem. Photobiol. B* **69,** 7–12
70. Morel, J. B., and Dangl, J. L. (1997) *Cell Death Differ.* **4,** 671–683
71. Asai, T., Stone, J. M., Heard, J. E., Kovtun, Y., Yorgey, P., Sheen, J., and Ausubel, F. M. (2000) *Plant Cell* **12,** 1823–1836
72. Stone, J. M., Heard, J. E., Asai, T., and Ausubel, F. M. (2000) *Plant Cell* **12,** 1811–1822
73. De Jong, A. J., Hoeberichts, F. A., Yakimova, E. T., Maximova, E., and Woltering, E. J. (2000) *Planta* **211,** 656–662
74. Mackey, D., Belkhadir, Y., Alonso, J. M., Ecker, J. R., and Dangl, J. L. (2003) *Cell* **112,** 379–389
75. Stone, S. L., Hauksdóttir, H., Troy, A., Herschleb, J., Kraft, E., and Callis, J. (2005) *Plant Physiol.* **137,** 13–30
76. Lin, S. S., Martin, R., Mongrand, S., Vandenabeele, S., Chen, K. C., Jang, I. C., and Chua, N. H. (2008) *Plant J.* **56,** 550–561
77. Goyal, L., McCall, K., Agapite, J., Hartwieg, E., and Steller, H. (2000) *EMBO J.* **19,** 589–597
78. Woo, C. H., Le, N. T., Shishido, T., Chang, E., Lee, H., Heo, K. S., Mickelsen, D. M., Lu, Y., McClain, C., Spangenberg, T., Yan, C., Molina, C. A., Yang, J., Patterson, C., and Abe, J. (2010) *FASEB J.* **24,** 4917–4928
79. Benard, G., Neutzner, A., Peng, G., Wang, C., Livak, F., Youle, R. J., and Karbowski, M. (2010) *EMBO J.* **29,** 1458–1471
80. Broemer, M., and Meier, P. (2009) *Trends Cell Biol.* **19,** 130–140
81. Chang, J. H., Urbach, J. M., Law, T. F., Arnold, L. W., Hu, A., Gombar, S., Grant, S. R., Ausubel, F. M., and Dangl, J. L. (2005) *Proc. Natl. Acad. Sci. U.S.A.* **102,** 2549–2554
82. Collmer, A., Lindeberg, M., Petnicki-Ocwieja, T., Schneider, D. J., and Alfano, J. R. (2002) *Trends Microbiol.* **10,** 462–469
83. Lindgren, P. B., Peet, R. C., and Panopoulos, N. J. (1986) *J. Bacteriol.* **168,** 512–522
84. Lorrain, S., Vailleau, F., Balagué, C., and Roby, D. (2003) *Trends Plant Sci.* **8,** 263–271
85. Yu, I. C., Parker, J., and Bent, A. F. (1998) *Proc. Natl. Acad. Sci. U.S.A.* **95,** 7819–7824